Bioorganic & Medicinal Chemistry 20 (2012) 1961–1972

Contents lists available at SciVerse ScienceDirect

Bioorganic & Medicinal Chemistry

journal homepage: www.elsevier.com/locate/bmc

Biochemical and transcriptional profiling to triage additional activities in a series of IGF-1R/IR inhibitors

Petra Ross-Macdonald [a,*], Heshani de Silva [a], Vishal Patel [a], Amy Truong [a], Aiqing He [a], Isaac Neuhaus [b], Charles Tilford [b], RuiRu Ji [b], Nathan Siemers [b], Ann Greer [c], Joan Carboni [c], Marco Gottardis [c], Krista Menard [c], Frank Lee [c], Marco Dodier [d], David Frennesson [d], Anthony Sampognaro [d], Mark Saulnier [d], George Trainor [d], Dolatrai Vyas [d], Kurt Zimmermann [d], Mark Wittman [d]

[a] Applied Genomics, Bristol-Myers Squibb Research and Development, Hopewell, NJ 08534, USA
[b] Bioinformatics, Bristol-Myers Squibb Research and Development, Hopewell, NJ 08534, USA
[c] Oncology Discovery Biology, Bristol-Myers Squibb Research and Development, Princeton, NJ 08540, USA
[d] Oncology Chemistry, Bristol-Myers Squibb Research and Development, Wallingford, CT 06492, USA

ARTICLE INFO

Article history:
Available online 6 November 2011

Keywords:
Kinase
IGF-1R
RNA profiling
Chemigenomics

ABSTRACT

Therapeutic development of a targeted agent involves a series of decisions over additional activities that may be ignored, eliminated or pursued. This paper details the concurrent application of two methods that provide a spectrum of information about the biological activity of a compound: biochemical profiling on a large panel of kinase assays and transcriptional profiling of mRNA responses. Our mRNA profiling studies used a full dose range, identifying subsets of transcriptional responses with differing EC_{50}s which may reflect distinct targets. Profiling data allowed prioritization for validation in xenograft models, generated testable hypotheses for active compounds, and informed decisions on the general utility of the series.

1. Introduction

Most kinase inhibitors target the conserved ATP binding site, creating an inherent challenge of specificity against the circa 512 kinases in the human genome. In response, methods to broadly profile these activities have been developed, including several commercially available biochemical panels,[1] and a reference collection of transcriptional profiling data.[2] We now have more information about the spectrum of clinically-applied kinase inhibitors than was available when they were originally developed.

Multi-kinase activities have sometimes proven useful; dasatinib (Sprycel) is approved as a BCR-ABL inhibitor for the treatment of CML,[3] but is also under clinical investigation as a SRC inhibitor for several indications,[4] while recent work suggests that dasatinib's activity against DDR2 may be relevant in NSCLC.[5] Crizotinib was originally developed as a relatively specific c-Met inhibitor,[6] but its approval process has been accelerated by its rapid application to cancers containing a recently identified second target: oncogenic fusions to the ALK kinase.[7] Nonetheless, for each such success story, there must be cases where additional activities have contributed to dose-limiting toxicity and led to clinical failure.

In developing or elaborating a targeted agent, the spectrum of bioactivity naturally varies, requiring choices on which additional properties might be advantageous to retain. The activities are relatively easy to measure, but the challenge is to use this information intelligently. We know little about the function of the majority of kinases, and even less about possible synergies in certain combinations. In vivo testing is a key step in establishing efficacy and toxicity, but the expense precludes testing more than a subset of the possible candidates. In the face of such uncertainty, one strategy is to identify and prioritize compounds with the minimal spectrum necessary to produce the in vitro effect. A second strategy is to ensure that compounds tested in vivo represent the full range of activities in possible candidates. Both strategies require interpreting the broad information on candidates that is now typically gathered during development of a targeted agent.

For example, IGF-1R is an oncology drug target because growth factor signaling through this receptor activates relevant mitogenic and antiapoptotic pathways.[8] During our development of a targeted IGF-1R/IR agent, data was gathered from both IGF-1-dependent and -independent cell lines, and inhibitory activity was measured against multiple kinases. We describe the use of such profiling results to triage a series of IGF-1R inhibitor candidates that had increased potency in non-IGF-1R-dependent models relative to our ultimate clinical candidate, the IGF-1R/IR inhibitor BMS-754807.[8]

* Corresponding author. Tel.: +1 609 818 7118; fax: +1 609 818 6935.
E-mail address: petra.rossmacdonald@bms.com (P. Ross-Macdonald).

0968-0896/$ - see front matter © 2011 Elsevier Ltd. All rights reserved.
doi:10.1016/j.bmc.2011.10.090

2. Results

2.1. Chemistry

Synthesis of BMS-754807 (compound **1**) has previously been described.[9] Experimental compounds **5**–**17** were prepared according to Scheme 1, starting from the previously described pyrrolotriazine **2**.[9] SNAr displacement of the chloride with (*R*) or (*S*)-4-F proline provided **3a** and **3b**. The resulting acids were generally converted to the corresponding methyl esters, **4a** and **4b** using EDC. Amides were generally prepared by reaction of the methyl esters with the Magnesium salt of the requisite heterocyclic amine in THF to provide the corresponding amides. Some of the less nucleophilic amines did require heating. Amide **10** was most efficiently

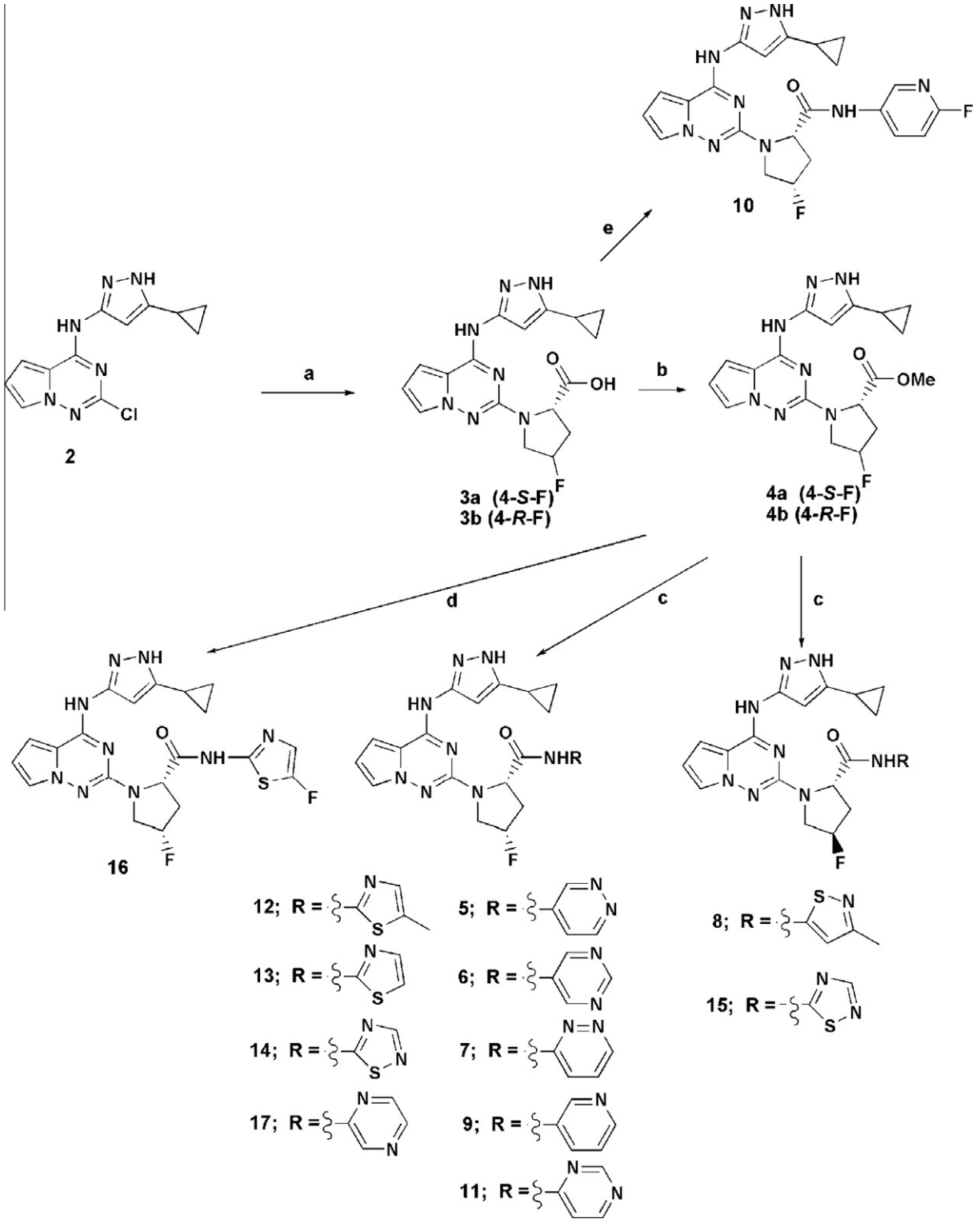

Scheme 1. Synthesis routes for experimental compounds in fluoroproline series (compounds **5**–**17**). Reagents and Conditions: (a) (*R*) or (*S*)-4-F proline, Huenig's base, 5 M NaOH, NMP, 135 °C; (b) EDC, N-Me morpholine, HOBT, MeOH, rt; (c) *i*PrMgCl, RNH_2, THF, 0 °C to rt; (d) RNH_2, iBu_3Al, toluene, 50 °C; (e) PPAA, NMM, rt.

prepared from the acid **3a** using PPAA. Alternatively, amide **16** was prepared from the methyl ester **4a** using the aluminate salt of the fluorothiazole.

2.2. Cellular cytotoxicity assays

In cellular assays of IGF-1R/IR-dependent models, such as the IGF-1R-Sal cell line, compound **1** inhibits IGF-1R signalling and shows antiproliferative activity at circa 10 nM.[8] In other contexts, its EC_{50} (concentration required to induce a 50% effect) is around 500 nM (Table 1), reflecting the selective biochemical profile of this kinase inhibitor.[8]

The fluoroproline compounds **5–17** retained activity against IGF-1R but also typically showed enhanced anti-proliferative activity in multiple non-IGF-1R dependent cell lines. For several compounds, cytotoxicity EC_{50} values as low as 20–30 nM were observed (see Table 1, where compounds are ranked by EC_{50} in A459 cells). Since this fluoroproline series was only one of several IGF-1R/IR inhibitor chemotypes available to explore, a further series of profiling assays was necessary to triage an informative subset for in vivo xenograft assays.

2.3. Triage using biochemical spectrum assay profiling

The KINOMEscan service uses bead-based competition assays and provides data in a reference form as the remaining percentage of signal relative to a control treatment.[10] A signal of 5% or less at in a KINOMEscan assay at 1 μM correlates with biochemical EC_{50}s below 100 nM in traditional assay formats (Table 1). Against a panel of 385 kinases (Table S1), compound **1** at 1 μM inhibits 12 kinases (3% of the panel) to less than 1% of control value. Compounds **1** and **5–17** were also profiled at a 1 μM dose against a panel of up to 384 kinases, where they displayed a greatly expanded biochemical activity profile (Table 1 and Table S1). Kinase targets that might be expected to have immediate relevance to the anti-proliferative activity include Src, CDK7, Aurora and AMPK kinase family members, but many additional kinases of unknown cellular function were also now inhibited. The number of additional kinases did not directly correlate with cytotoxicity, for example, the most potent compound, **17**, has fewer activities than compound **9**. Hierarchical clustering of the KINOMEscan profiling data shows 3 major groupings: the least cytotoxic compounds (compounds **5–8**) group with compound **1**, three compounds (**10**, **11** and **12**) group with an intermediate profile, and the remaining compounds including **9** have the broadest spectrum (Fig. 1A).

To place the additional kinase activities in the context of structural relationships, we visualized the data on a family tree that accurately reflects degree of homology across the kinome (Fig. 1B). This representation allows us to balance the likely biological impacts in our candidate selection. For example, while compound **9** has many additional activities relative to a compound with similar cytotoxicity, **10**, they are largely confined to targets in the Receptor Tyrosine Kinase family and thus may only be of relevance in specific transformation models. Conversely, the compounds that quite selectively impact essential kinases such as CDK7 in the CMGC family may be broadly deleterious to cell viability,[11] and we must ensure that further testing does not over-represent such activities.

2.4. Triage using transcriptional profiling

The nine fluoroproline compounds with the lowest cytotoxicity EC_{50} values for the A549 cell line (**9–17**) were selected for a transcription profiling analysis that compared their effects in a four-hour treatment with those of compound **1**. We used a 12-point dose regimen modeled on the dose-response cytotoxicity assay, which is amenable to identifying transcriptional responses with EC_{50}s in the interval between 0.54 nM and 10 μM. (Two samples failed for compound **15**). For each probeset on the Affymetrix array, the 12 intensity values for each treatment were processed with the SDRS algorithm to identify those with a sigmoidal dose response ('response transcripts').[12]

For each compound, the number of response transcripts meeting $P < 0.05$ and a 1.5-fold change is indicated in Table 2 (with a full report in Table S2). However, a more useful overview is provided by the visualization in Figure 2, which shows the number of response transcripts (intensity) as a function of both dose (X axis) and statistical significance (Y axis). Thus for compound **1**, in this four hour treatment, a significant and co-ordinated transcriptional response is not observed until treatment is in the micromolar dose range. There is no set of transcriptional responses around the EC_{50} dose for cellular IGF-1R inhibition (10 nM,[8]), reflecting the IGF-1 independence of A549. There are also no transcriptional responses around the cytotoxic EC_{50} dose of compound **1** (484 nM in A549 cells) that meet the statistical criteria, indicating that impact on the kinase target responsible for its cytotoxicity does not have a strong transcriptional readout at this early time point. We have previously observed this phenomenon in dose-response analysis of dasatinib (cytotoxic EC_{50} 20 nM in A549 cells), finding many response transcripts with EC_{50}s of 20 nM at 20 h, but very few at 4 h.[12] The corollary of this observation is that, if the cytotoxicity of the fluoroproline series at circa 100 nM is due to the same kinase target that is impacted by compound **1** at 500 nM, we would not expect to see a transcriptional readout at 100 nM in treatments with **9–17** either.

For the majority of the fluoroproline compound series, the transcriptional dose responses are also predominantly in the micromolar dose range (Fig. 2 and Table 2). Compounds **14** and **17** are exceptions, since they have a set of multiple transcriptional responses with EC_{50}s below 1 μM. To ask whether this represents a distinct kinase activity of these two compounds or a potency shift for a shared target, we closely examined the transcriptional responses for the set of 285 probesets that have a dose response for compounds **14** and/or **17** with an EC_{50} of less than 1 μM (also $P < 0.001$, >1.3-fold change, signal of 3× background; Table S2). We found that 19 of these also meet $P < 0.05$ for a dose response in all ten compounds, including compound **1** (Fig. 3A), while 39 meet $P < 0.05$ for a dose response in all nine compounds in the fluoroproline series (Fig. 3B). These probesets represent an activity or activities that are common to compounds **9–17**, and show EC_{50}s ranging from 1 nM to the high micromolar range. The activity is not the cytotoxic target that compounds **9–17** share with compound **1**, since these responses are largely absent with compound **1**. There is no obvious correlation between the EC_{50}s for these transcriptional responses and the cytotoxic EC_{50}s or the rank order of potency for **9–17**. Following the strategy of prioritizing compounds with the minimal spectrum necessary to produce the in vitro effect, we would seek to minimize representation of such activities in compounds selected for further studies. One example is compound **9**, where these responses do not occur until a micromolar dose.

2.5. Analysis of a distinct transcriptional response to compound 14

Compound **14** shows cytotoxicity at doses below 1 μM across 59 cell lines tested (Table S3) indicating that it potently inhibits a kinase or kinases involved in a fundamental cellular process. Among the 285 probesets that are regulated by compounds **14** and/or **17** with an EC_{50} of less than 1 μM (and $P < 0.001$, >1.3-fold change, signal of 3× background) we identified 67 probesets that meet those criteria for compound **14**, but do not have a dose response curve that meets $P < 0.05$ with less potent compounds such

Table 1
Chemical structure; KINOMEscan versus in vitro kinase assays for IGF-1R and Aurora B; anti-proliferative EC_{50} in three cell lines; KINOMEscan assay data summary.

Compound	Structure	4F (R/S)	IGF-1R		Aurora B		Proliferation			KINOMEscan	
			% Control	IC_{50}, nM	% Control	IC_{50}, nM	IGF-Sal EC_{50}, nM	A549 EC_{50}, nM	HCT-116 EC_{50}, nM	# kinases in test panel	# of kinases with <1% of control signal (% of panel)
1			0.6	3	6	23	9	484	509	385	12 (3%)
5	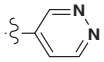	S	0.3	7	12	123	11	1000	806	384	7 (2%)
6	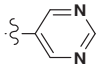	S	0.3	7	9	27	60	846	603	384	4 (1%)
7		S	0.4	15	5	13	146	383	413	384	13 (3%)
8	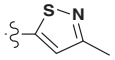	R	0.7	1	5	nd	6	145	57	358	9 (3%)
9		S	0.3	6	0.2	6	34	124	59	358	59 (16%)
10	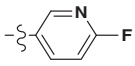	S	0.3	3	2	9	3	82	82	384	30 (8%)
11	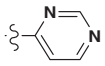	S	0.2	8	5	15	10	76	75	384	36 (9%)
12	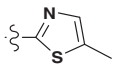	S	0.2	3	1	8	8	73	86	384	31 (8%)
13		S	0.1	4	0.4	7	27	72	90	384	58 (15%)
14		S	0.3	2	0.1	8	6	52	59	358	53 (15%)
15		R	0.5	3	0.2	nd	11	27	37	289	47 (16%)
16	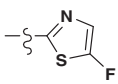	S	0.1	2	1	8	5	20	33	384	70 (18%)
17		S	0.2	2	1	9	2	19	18	384	44 (11%)

as **9** and **10**. Most of the 67 responses have a co-ordinated EC_{50} of around 300 nM (Fig. 3C), indicating a target inhibition EC_{50} at this dose. These transcriptional responses were also present in compound **15**, the enantiomer of **14**, although with less clarity due to the lack of two dose points in this dataset. Only one of the 67 has an EC_{50} of less than 1 μM with the more potent compound **17**. These 67 responses reveal a distinct impact of compound **14** in the sub-1 μM range that we sought to clarify.

The 67 probesets were submitted to a gene set enrichment analysis[13] which revealed an overrepresentation for nuclear proteins (corrected *P* value 4.04×10^{-5}; 43 probesets represent members of GO category 0005634: Nucleus[14]) and for proteins involved in nucleic acid metabolism (corrected *P* value 0.016; 18 probesets are members of MSigDB: NUCLEOBASE/NUCLEOSIDE/NUCLEOTIDE AND NUCLEIC ACID METABOLIC PROCESS[15]). We also submitted the 67 proteins represented by the probesets to Kinase Enrichment Analysis.[16] A significant enrichment for substrates of CDK2 was observed (9 proteins, *P* value 0.002), including splicing factor SFRS2 and the kinase PRPF4B. These are among several regulated genes that are involved in mRNA processing, including SFRS4 and another CMGC-family kinase, SRPK2 (Fig. 4). In KINOMEscan assays (Supplementary Table 1), compound **14** has no direct activity on CDK2, PRPF4B or SRPK2, and we could not identify one kinase that accounted for the unique activity. The unique transcriptional readout may represent a potency difference that could not be scored in the single-dose KINOMEscan assay, or a combination of kinase targets, or a target such as one of the twelve CMGC kinases not represented in this KINOMEscan panel. While we could not determine the specific target of compounds **14** and **15** from profiling assays, we have an insight on one affected process (CDK2-regulated mRNA processing) and can judge whether or not we wish to evaluate that impact in vivo.

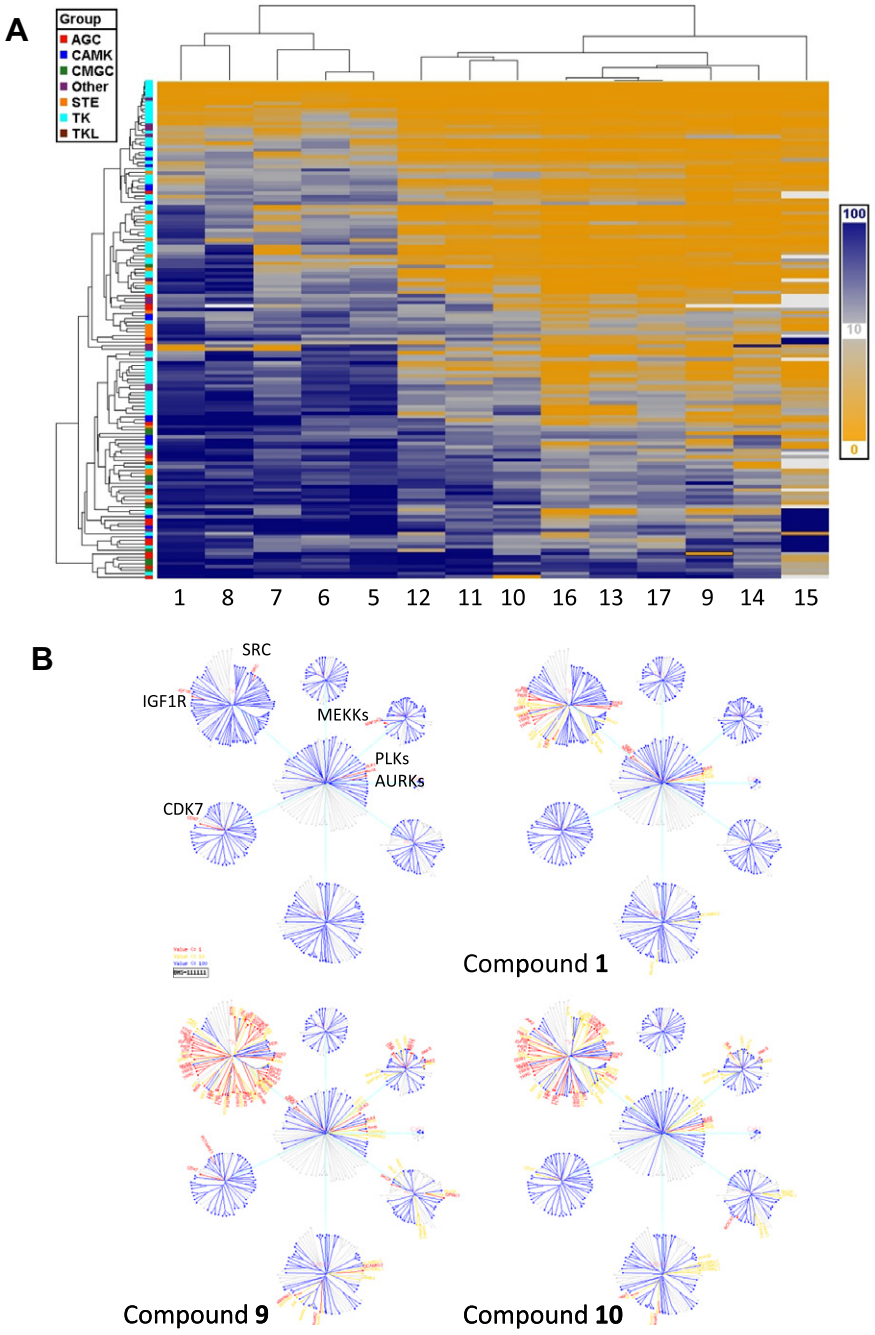

Figure 1. Characterization of the Kinome inhibition profile of each compound. (A) Heirarchical clustering of data from the KINOMEscan platform; the 149 kinase targets for which at least one compound has activity <10% of control value are represented. (B) Results of biochemical assays performed on the KINOMEscan platform are color coded over the respective kinase in a topological layout that reflects structural homology of kinases. Red indicates the remaining percentage of signal relative to a control treatment was <1%, gold indicates remaining signal <10%, and all other assays performed are indicated in blue.

Table 2
Quantification of the dose-responsive transcriptional effects

Identifier	Response transcripts, P <0.05, Fold >1.5	Response transcripts, P <0.001, Fold >1.3, EC_{50} <1 μM, B >16
1	613	7
9	748	12
10	988	41
11	583	22
12	614	11
13	1359	114
14	2121	190
15	1739	63
16	1068	41
17	1165	119

2.6. Comparison to the transcriptional response profile for CDK9/RNA polymerase II inhibition

In the CMGC kinase group, several of the compounds in the fluoroproline series showed strong and selective activity for CDK7 (Fig. 1, Supplementary Table 2). CDK7 has been proposed as an oncology target, based on its 'master regulator' activity over cell cycle CDKs 1, 2, 4 and 6 and its critical function in initiation of transcription by RNA polymerase II.[11] We considered the possibility that CDK7 inhibition underlay the cytotoxic effect of some fluoroproline compounds. To investigate the relationship between inhibition of RNA polymerase II (via CDK7) and the transcriptional

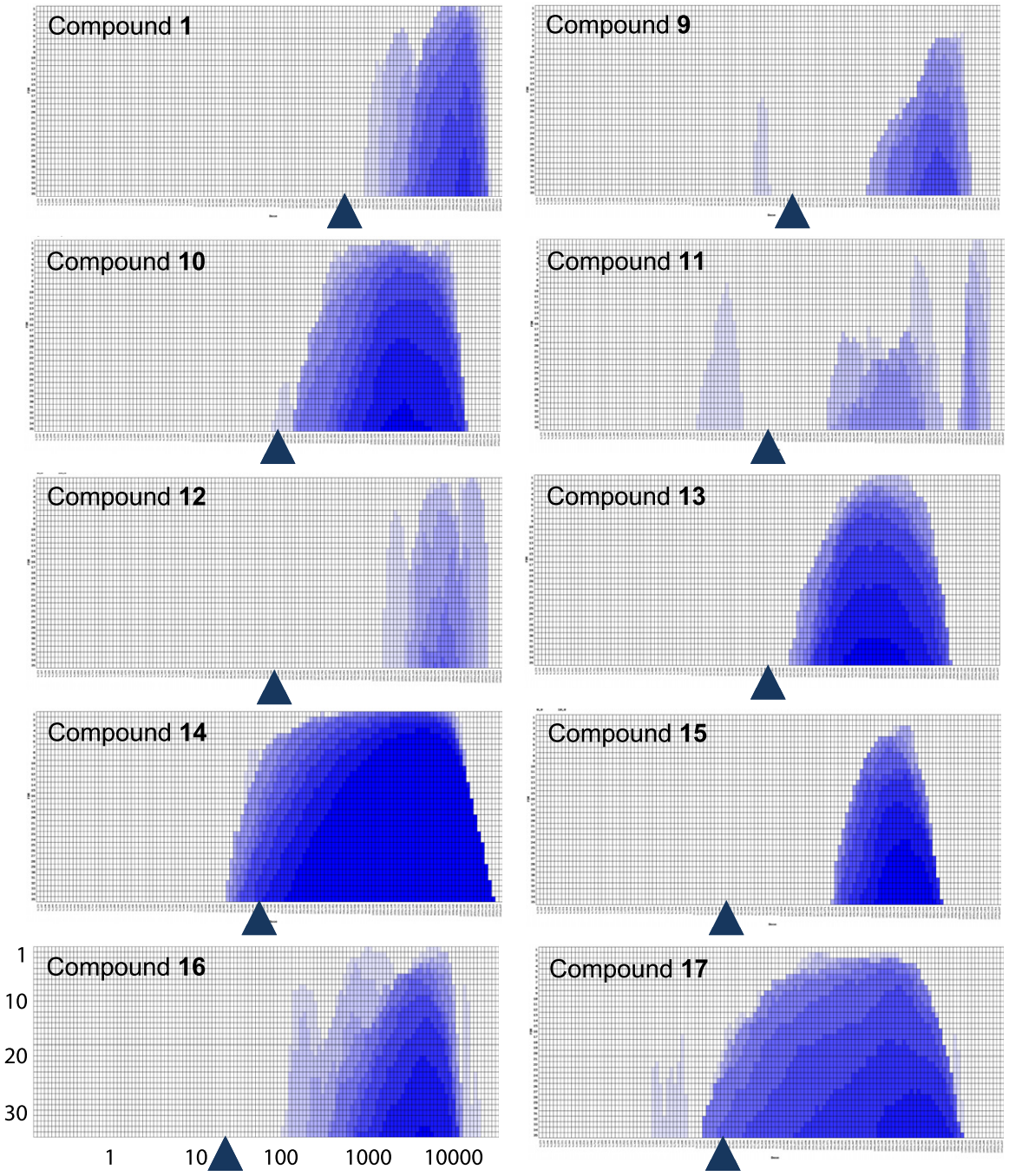

Figure 2. Characterization of the overall transcriptional response to each compound across the dose range. Each heatmap displays the number of probesets whose goodness of fit to a sigmoidal curve passes the given false discovery rate (FDR) criterion at the given dose point. The horizontal axis contains a dose range (the EC_{50} values evaluated in the SDRS algorithm), and the vertical axis contains a Probability range, with one row for each of the 35 FDR criteria applied. Color intensity reflects the number of probesets on a two-fold scale, that is, the increasing color saturation represents '2 or more probesets', '4 or more', '8 or more', etc. The filled arrowhead indicates the cytotoxic EC_{50} for that compound in the A549 cell line.

effects of the series, we performed a comparison with flavopiridol. Flavopiridol is a potent and relatively specific inhibitor of CDK9,[17] and acts on RNA polymerase II at the step immediately following CDK7 action, arresting most RNA polymerase II-dependent transcription.[18] Under the same conditions as our experimental treatments, we identified 1180 probesets that are regulated by flavopiridol treatment (Table S3). Highly concordant EC_{50} values between 30 and 100 nM were observed for these responses (Fig. 5A), which reflects the compound's inhibitory EC_{50} for CDK9 (30 nM).[17] In contrast, the same probesets show a divergent set of EC_{50} values within in each treatment in the fluoropr-

oline series, with the majority of EC_{50}s lying in the micromolar range (Fig. 5B). For example, compound **14** was the most potent CDK7 inhibitor in the KINOMEscan assay, and does share many of the flavopiridol response transcripts. However only a subset are regulated at

sub-micromolar doses of compound **14**, indicating that the antiproliferative effect in the sub-micromolar range is not related to a general effect on RNA polymerase II via CDK7. The majority of the flavopiridol response transcripts are sharply regulated by compound **14** at EC_{50} of circa 3 μM, which is presumably where its inhibition of CDK7 occurs.

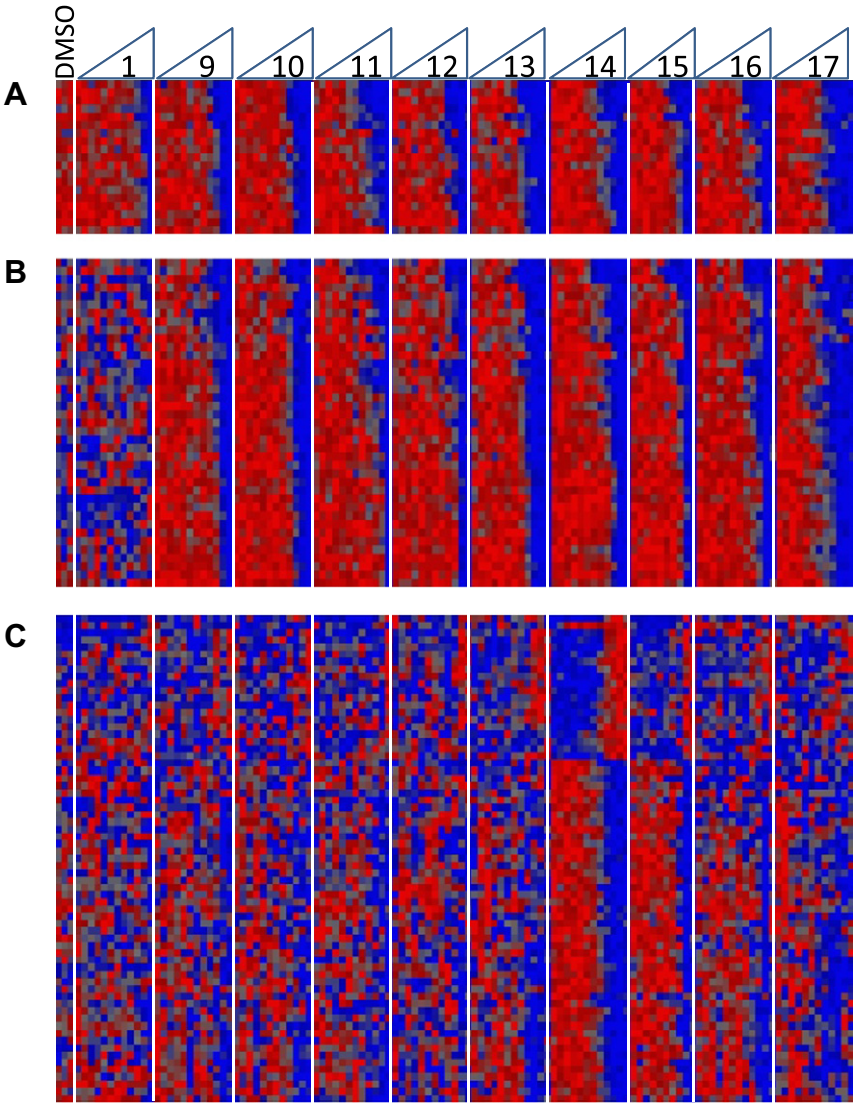

Figure 3. Transcriptional responses of selected probesets across dose ranges of compound **1** and nine fluoroproline IGF-1R/IR inhibitors. For each treatment, the highest dose point is 30 μM, with a 3-fold dilution extending to the left. For the 12 samples that comprise each treatment (10 for Compound **15**), actual intensity data was scaled from 0 to 1. Data for three DMSO vehicle-treated samples was scaled with data for compound **1**. (A) Nineteen probesets that meet P <0.05 for a sigmoidal response in all ten compounds. (B) 39 probesets that meet P <0.05 for a sigmoidal response in all nine compounds in the fluoroproline series. (C) 67 probesets that meet P <0.001 for a sigmoidal response and fold change >1.3 with compound **14** at EC_{50} <1 μM, but do not meet P <0.05 for a sigmoidal response with compounds **9** and **10**.

2.7. In vivo analysis using an HCT-116 xenograft tumor model

Based on the biological profiling results described above, we prioritized five compounds for testing in vivo. Four compounds were selected based on the strategy of having the minimal spectrum necessary to produce the in vitro effect: relative to the selective IGF-1R/IR inhibitor **1**, compounds **10, 11** and **12** have the least additional activity in KINOMEscan assays, while compound **9** (along with **11** and **12**) has the least additional activity in transcriptional assays. One compound was chosen based on the strategy of ensuring that compounds tested in vivo represent the range of activities in possible candidates: compound **14** was included to investigate its sub-micromolar activity, which may represent a novel target space.

All five compounds were dosed in a xenograft tumor model of the HCT-116 colon epithelial cell line (Table 3). The ranking of in vitro potency of the compounds did not correlate with their in vivo activity. Such lack of correlation is not unusual, and illustrates the impact of pharmacokinetic/pharmacodynamic factors and the importance of testing several candidates to get true representation. The most active compound was **10**, which showed 69% tumor growth inhibition (TGI) at a dose level of 25 mg/kg daily. Compound **9** was also active, showing 55% TGI at 50 mg/kg.

3. Discussion

Compounds such as the cytotoxic fluoroproline compound series **5–17** are often generated during optimization of a targeted agent. Their broad activity suggests a fundamental cellular target (most likely a kinase, but other activities have been demonstrated for kinase inhibitors[19]), which carries the potential for dose-limiting toxicity. We wished to make informed decision about the utility of the series using profiling data to select a representative test set for a small in vivo evaluation. These multivariate datasets provide a new challenge of how to best use the information for decision-making in such a project. Our representative set prioritized four active compounds that had minimal additional activities. This strategy is only one possibility: with other goals we could have

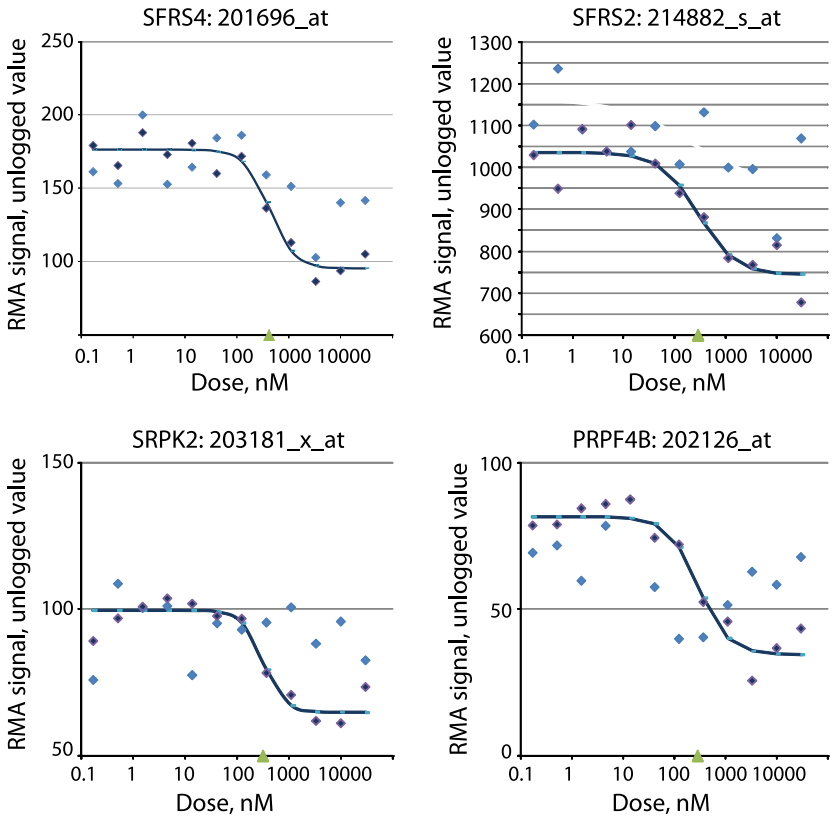

Figure 4. Transcriptional responses of four genes involved in mRNA processing. The filled diamond markers show the actual signal intensities for the probeset indicated, across dose ranges of compound **10** (light blue) and compound **14** (dark blue). For compound **14**, the sigmoidal dose response curve with best fit to experimental data is shown (dark blue line). The EC_{50} for this curve is indicated by a green arrowhead on the X-axis. For compound **10**, there is no sigmoidal dose response curve that fits the data with P <0.05.

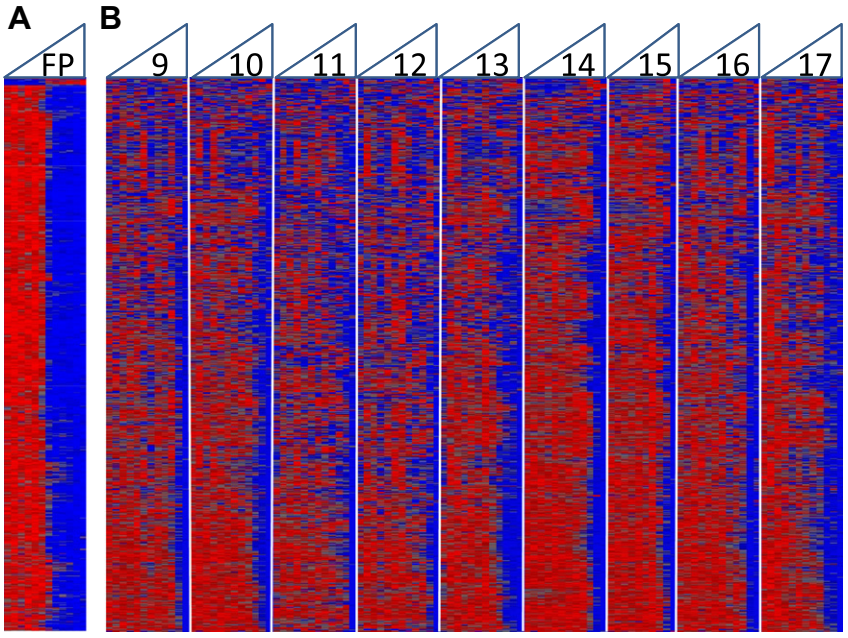

Figure 5. Transcriptional responses of flavopiridol-regulated probesets across dose ranges of flavopiridol and nine fluoroproline IGF-1R/IR inhibitors. For each treatment, the highest dose point is 30 μM, with a 3-fold dilution extending to the left. For the 12 samples that comprise each treatment (10 for compound **15**), actual intensity data was scaled from 0 to 1. (A) Flavopiridol treatment intensity data for 1180 probesets that meet P <0.05 for a sigmoidal response and fold-change >1.5 in flavopiridol treatment. (B) Data for same 1180 probesets in treatments with the fluoroproline compounds.

chosen compounds representing the most diverse profiles, or based on specific kinase targets. From our test set, we identified compound **10** as a potent antiproliferative agent in vivo, with a tractable kinase target spectrum (Fig. 1) and a transcriptional effect

Table 3
Summary of HCT-116 xenograft tumor growth inhibition (TGI) responses at 14 days

Identifier	Dose, mg/kg	Efficacy, % TGI
1	50	44
9	50	55
10	25	69
11	50	19
12	25	Inactive
14	50	15

in the submicromolar range (Fig. 2) that may be relevant to its in vivo activity. We judged that the test set had given the fluoroproline series the best opportunity to reveal value, but ultimately pursued clinical development with the more selective kinase inhibitor, compound **1**.[8]

4. Experimental section

4.1. Compound preparation

4.1.1. (2*S*,4*S*)-1-(4-(5-Cyclopropyl-1*H*-pyrazol-3-ylamino)pyrrolo[1,2-*f*][1,2,4]triazin-2-yl)-4-fluoropyrrolidine-2-carboxylic acid (3a)

(2*S*,4*S*)-4-Fluoropyrrolidine-2-carboxylic acid hydrochloride (3.39 g, 20.0 mmol) was suspended in NMP (25 mL) to which was added 5 M NaOH (4.00 mL, 20.0 mmol), followed by DIPEA (1.92 mL, 11.0 mmol) and 2-chloro-*N*-(5-cyclopropyl-1*H*-pyrazol-3-yl)pyrrolo[1,2-*f*][1,2,4]triazin-4-amine (1.37 g, 5.00 mmol). The reaction mixture was heated to 135 °C for 3 d, and then cooled to room temperature. The reaction was diluted with water (500 mL) and washed with EtOAc (2 × 250 mL). The organic layers were discarded, and the aqueous layer was adjusted to pH 2–3 with 1 N HCl and extracted with EtOAc (2 × 250 mL). The combined extracts were washed with brine (250 mL), dried ($MgSO_4$), filtered, and concentrated in vacuo. The resulting residue was shaken vigorously with water (500 mL), and a precipitate was removed by vacuum filtration. The solids were again vigorously shaken with water (150 mL) and dried via vacuum filtration to afford slightly impure acid (974 mg, 52%) with an LC/MS $M^+ + 1 = 372$.

4.1.2. (2*S*,4*S*)-Methyl 1-(4-(5-cyclopropyl-1*H*-pyrazol-3-ylamino)pyrrolo[1,2-*f*][1,2,4]triazin-2-yl)-4-fluoropyrrolidine-2-carboxylate (4a)

Slightly impure (2*S*,4*S*)-1-(4-(5-cyclopropyl-1*H*-pyrazol-3-ylamino)pyrrolo[1,2-*f*][1,2,4]triazin-2-yl)-4-fluoropyrrolidine-2-carboxylic acid (900 mg, approx. 2.19 mmol) was dissolved in MeOH (22 mL) and cooled to 0 °C. Acetyl chloride (1.56 mL, 21.9 mmol) was added, and the reaction was stirred at 0 °C for several minutes before warming to room temperature. After 16 h, the reaction was concentrated in vacuo. The residue was diluted with EtOAc (300 mL) and washed with saturated aqueous $NaHCO_3$ (300 mL), water (300 mL) and brine (150 mL). The organics were dried ($MgSO_4$), filtered, and concentrated in vacuo. The compound was purified by silica gel flash chromatography (0–50% 90:10:1 [CH_2Cl_2/MeOH/conc NH_4OH]/CH_2Cl_2) to give methyl ester (564 mg, 66%) with an LC/MS $M^+ + 1 = 386$.

4.1.3. (2*S*,4*R*)-Cyclopropyl-1H-pyrazol-3-ylamino)pyrrolo[1,2-f][1,2,4]triazin-2-yl)-4-fluoropyrrolidine-2-carboxylic acid (3b)

A mixture of the chloropyrrolotriazine 2 (1.77 g, 6.43 mmol) and (2*S*,4*R*)-4-fluoropyrrolidine-2-carboxylic acid (1.989 g, 14.9 mmol) in a 48 mL pressure bottle is treated with NMP (20 mL) followed by *N*,*N*-diisopropylethylamine (1.43 mL, 8.20 mmol). To this stirred mixture is then added 5 M NaOH (2.88 mL, 14.4 mmol). The reaction is flushed with nitrogen, sealed, and heated at 115 °C for 45 h, at 135 °C for 24 h, and finally at 117 °C for 15 h. The crude reaction mixture is poured into water (300 mL) and dichloromethane (200 mL). The organic layer is removed and the aqueous layer is extracted with additional dichloromethane (3 × 50 mL). The water layer is treated with aqueous 1.0 N HCl (18–20 mL,) to pH 2–3 and extracted with ethyl acetate (2 × 400 mL). The ethyl acetate layers were combined, washed with water (2 × 50 mL) and brine (50 mL), and dried (Na_2SO_4). Concentration in vacuo gives the title compound (1.97 g) as a solid which is 70% pure by HPLC and is used as is for the reactions described below; MS: 372 $(M+H)^+$, LC/MS ret. t = 1.83 min; HPLC (Method A) ret. t. = 6.8 min; 300 MHz ^{1}H NMR (CD_3OD) δ 7.38 (s, 1H), 6.91–6.81 (m, 1H), 6.52–6.44 (m, 1H), 6.34 (s, 1H), 5.41 (d, 1H, J = 53.4 Hz), 4.73 (t, 1H, J = 8.1 Hz), 4.14–3.70 (m, 2H), 2.87–2.64 (m, 1H), 2.44–2.21 (m, 1H), 2.00–1.86 (m, 1H), 1.06–0.92 (m, 2H), 0.88–0.72 (m, 2H).

4.1.4. (2*S*,4*R*) Methyl 1-(4-(5-cyclopropyl-1H-pyrazol-3-ylamino)pyrrolo[1,2-f][1,2,4]triazin-2-yl)-4-fluoropyrrolidine-2-carboxylate (4b)

To a solution of the acid (2.21 g, 4.7 mmol) in 40 ml methanol were added 1-hydroxybenzotriazole (1.08 g, 8 mmol), *N*-methylmorpholine (1.76 ml, 16 mmol), and 1-[3-(dimethylamino)propyl]-3-ethylcarbodiimide hydrochloride (1.53 g, 8 mmol). The mixture was stirred at ambient temperature. After a total time of 4 h the mixture was concentrated, dissolved in ethyl acetate, washed with a saturated aqueous $NaHCO_3$ solution, water and brine, dried over $MgSO_4$, filtered and concentrated. The product was purified by chromatography on a Horizon Biotage system, using a 40-M cartridge (conditioned with 95% dichloromethane + 5% ethyl acetate) and eluted with a gradient from 5% ethyl acetate in dichloromethane to 100% ethyl acetate. 997.8 mg of the title compound were isolated. LC–MS m/e = 385, $[M+H]^+$.

4.1.5. General procedure A

The amine (1.5 mmol) was dissolved in 5 ml THF and the solution cooled to 0 °C. Isopropyl magnesium chloride (2.0 M solution in THF, 1.35 ml, 2.7 mmol) was added and the mixture stirred for 5 min. A solution of (2*S*,4*R*)-methyl 1-(4-((5-cyclopropyl-1H-pyrazol-3-yl)amino)pyrrolo[2,1-f][1,2,4]triazin-2-yl)-4-fluoropyrrolidine-2-carboxylate (99 mg, 0.256 mmol) in 5 ml THF was added and stirring at 0 °C continued for 1 h, then 1 h at ambient temperature. The reaction mixture was poured into a 1 + 3 mixture of aq NH_4Cl solution and aq $NaHCO_3$ solution and extracted with ethyl acetate. The organic layer was washed with brine, dried over $MgSO_4$, filtered and concentrated in vacuum. The crude was purified by preparative HPLC (Waters Sunfire column 30 × 150 mm, water/CH_3CN gradient with 0.1% TFA). Product containing fractions were filtered through a Waters MCX cartridge (1 g). The cartridge was washed with MeOH and the product eluted with a 1 + 1 mixture of dichloromethane and 2 M NH_3 in MeOH. Evaporation of volatiles gave the desired product.

4.1.6. General procedure B

Isopropylmagnesium chloride (2.0 M solution in THF, 6.23 mL, 12.5 mmol) was added to a solution the amine(13.0 mmol) in THF (90 mL). After stirring for several minutes, the solution was quickly transferred to a flask containing (2*S*,4*S*)-methyl 1-(4-((5-cyclopropyl-1H-pyrazol-3-yl)amino)pyrrolo[2,1-f][1,2,4]triazin-2-yl)-4-fluoropyrrolidine-2-carboxylate (2.59 mmol). The reaction was stirred overnight at rt, then quenched with sat aq NH_4Cl (150 mL). The mixture was extracted with EtOAc (150 mL), and the organics were washed with water (3 × 150 mL), dried ($MgSO_4$), filtered, and concentrated in vacuo. The residue was purified via a

silica gel column (0–35% 90:10:1 [CH_2Cl_2/MeOH/NH_4OH]/CH_2Cl_2), then by preparative HPLC (Waters Atlantis 30 × 100 mm, 0–70% 9:1 [MeOH/H_2O 0.1% TFA]/1:9 [MeOH/H_2O 0.1% TFA]). Product-containing fractions were concentrated on a Waters Oasis MCX cartridge, rinsed with MeOH, then eluted with 2 N NH_3/MeOH. The eluent was concentrated in vacuo to obtain the desired product.

4.1.7. (2*S*,4*S*)-1-(4-(5-Cyclopropyl-1*H*-pyrazol-3-ylamino) pyrrolo[1,2-*f*][1,2,4]triazin-2-yl)-4-fluoro-*N*-(pyridazin-4-yl)pyrrolidine-2-carboxamide (5)

Starting with pyridazin-4-amine, procedure B was followed to provide the desired product (23%): MS *m*/*z* = 447 (neg. mode). ^{1}H NMR (CD_3OD) δ 9.32 (dd, *J* = 2.6, 0.9 Hz, 1H), 8.93 (dd, *J* = 6.0, 1.0 Hz, 1H), 8.05 (dd, *J* = 5.8, 2.5 Hz, 1H), 7.41 (dd, *J* = 2.5, 1.5 Hz, 1H), 6.89–6.80 (m, 1H), 6.49 (dd, *J* = 4.5, 2.5 Hz, 1H), 6.19 (br s, 1H), 5.48–5.28 (m, 1H), 4.90–4.78 (m, 1H), 4.06–3.91 (m, 1H), 3.90–3.71 (m, 1H), 2.74–2.50 (m, 2H), 1.79–1.68 (m, 1H), 0.91–0.84 (m, 2H), 0.71–0.52 (m, 2H).

4.1.8. (2*S*,4*S*)-1-(4-(5-Cyclopropyl-1*H*-pyrazol-3-ylamino) pyrrolo[1,2-*f*][1,2,4]triazin-2-yl)-4-fluoro-*N*-(pyrimidin-5-yl)pyrrolidine-2-carboxamide (6)

Starting with pyrimidin-5-amine, procedure B was followed to provide the desired product (48%): MS *m*/*z* = 449. ^{1}H NMR (CD_3OD) δ 8.95 (s, 2H), 8.81 (s, 1H), 7.40 (d, *J* = 1.5 Hz, 1H), 6.85 (d, *J* = 3.3 Hz, 1H), 6.48 (dd, *J* = 4.3, 2.5 Hz, 1H), 6.26 (br s, 1H), 5.48–5.29 (m, 1H), 4.83–4.77 (m, 1H), 4.07–3.91 (m, 1H), 3.90–3.71 (m, 1H), 2.73–2.50 (m, 2H), 1.81–1.69 (m, 1H), 0.92–0.80 (m, 2H), 0.72–0.54 (m, 2H).

4.1.9. (2*S*,4*S*)-1-(4-(5-Cyclopropyl-1*H*-pyrazol-3-ylamino) pyrrolo[1,2-*f*][1,2,4]triazin-2-yl)-4-fluoro-*N*-(pyridazin-3-yl)pyrrolidine-2-carboxamide (7)

Starting with pyridazin-3-amine procedure B was followed to provide the desired product (43%): MS *m*/*z* = 447 (neg. mode). ^{1}H NMR (DMSO-d_6) δ 12.06 (br s, 1H), 10.76 (s, 1H), 10.31 (s, 1H), 8.95 (dd, *J* = 4.8, 1.5 Hz, 1H), 8.34–8.25 (m, 1H), 7.67 (dd, *J* = 9.1, 4.8 Hz, 1H), 7.46 (s, 1H), 7.13 (br s, 1H), 6.43 (dd, *J* = 4.3, 2.5 Hz, 1H), 6.33 (br s, 1H), 5.53–5.33 (m, 1H), 4.88 (d, *J* = 9.8 Hz, 1H), 3.94–3.71 (m, 2H), 2.78–2.55 (m, 1H), 2.54–2.39 (m, 1H), 1.68 (br s, 1H), 0.75 (d, *J* = 6.8 Hz, 2H), 0.64–0.42 (m, 2H).

4.1.10. (2*S*,4*R*)-1-(4-(5-cyclopropyl-1H-pyrazol-3-ylamino) pyrrolo[1,2-f][1,2,4]triazin-2-yl)-4-fluoro-N-(3-methylisothiazol-5-yl)pyrrolidine-2-carboxamide (8)

Starting with 5-amino-3-methyl-isothiazol hydrochloride, procedure A was followed to provide the desired product (68% yield). LC–MS m/e+ = 468 $[M+H]^+$, 500 MHz ^{1}H NMR (DMSO-d_6) δ 12.10 (s, 1H), 11.84 (s, 1H), 10.26 (s, 1H), 7.36 (s, 1H), 7.11 (s, 1H), 6.71 (s, 1H), 6.42 (s, 1H), 6.30 (s, 1H), 5.45 (d, 1H, *J* = 53.1 Hz), 4.77 (t, 1H, *J* = 8.1 Hz), 4.13 (dd, 1H, *J* = 13.7, 23.3 Hz), 3.98–3.75 (ddd, 1H, *J* = 36.9, 12.5, 2.5 Hz), 2.78–2.61 (m, 1H), 2.37–2.13 (m, 1H), 2.27 (s, 3H), 1.93–1.82 (m, 1H), 0.98–0.89 (m, 2H), 0.82–0.76 (m, 2H).

4.1.11. (2*S*,4*S*)-1-(4-(5-cyclopropyl-1H-pyrazol-3-ylamino) pyrrolo[1,2-f][1,2,4]triazin-2-yl)-4-fluoro-N-(pyridin-2-yl)pyrrolidine-2-carboxamide (9)

Starting with 2-amino pyridine, procedure B was followed to provide the desired product (532 mg, 45%): MS *m*/*z* = 446 (neg. mode). ^{1}H NMR (DMSO-d_6) δ 12.09 (br s, 1H), 10.34 (s, 1H), 9.79 (s, 1H), 8.24 (dd, *J* = 4.8, 1.0 Hz, 1H), 8.11 (d, *J* = 8.3 Hz, 1H), 7.81–7.73 (m, 1H), 7.47 (d, *J* = 2.0 Hz, 1H), 7.14 (br s, 1H), 7.08 (ddd, *J* = 7.3, 4.8, 1.0 Hz, 1H), 6.44 (dd, *J* = 4.4, 2.4 Hz, 1H), 6.32 (br s, 1H), 5.52–5.33 (m, 1H), 4.80 (d, *J* = 10.1 Hz, 1H), 3.94–3.72 (m, 2H), 2.74–2.38 (m, 2H), 1.80–1.65 (m, 1H), 0.79 (d, *J* = 8.6 Hz, 2H), 0.73–0.50 (m, 2H).

4.1.12. (2*S*,4*S*)-1-(4-(5-Cyclopropyl-1*H*-pyrazol-3-ylamino) pyrrolo[1,2-*f*][1,2,4]triazin-2-yl)-4-fluoro-*N*-(6-fluoropyridin-3-yl)pyrrolidine-2-carboxamide (10)

A mixture of (2*S*,4*S*)-1-(4-((5-cyclopropyl-1H-pyrazol-3-yl)amino)pyrrolo[2,1-f][1,2,4]triazin-2-yl)-4-fluoropyrrolidine-2-carboxylate (1.50 g, 4.04 mmol) and 6-fluoropyridin-3-amine (2.26 g, 20.2 mmol) was dissolved in NMM (10.5 mL) and cooled in an ice/water bath. 1-Propanephosphonic acid cyclic anhydride (50 wt % solution in EtOAc, 3.61 mL, 6.06 mmol) was slowly added. The reaction was stirred at rt for 90 min, then poured into sat aq $NaHCO_3$ (250 mL) and extracted with EtOAc (2 × 200 mL). The combined extracts were washed (250 mL water, then 150 mL brine), dried ($MgSO_4$), filtered, and concentrated in vacuo. The residue was purified via silica gel chromatography (0–35% 90:10:1 [CH_2Cl_2/MeOH/NH_4OH]/CH_2Cl_2) then preparative HPLC (Waters Atlantis 30 × 100 mm, 0–73% 9:1 [MeOH/H_2O 0.1% TFA]/1:9 [MeOH/H_2O 0.1% TFA]). Product-containing fractions were concentrated on a Waters Oasis MCX cartridge, rinsed with MeOH, then eluted with 2 N NH_3/MeOH. The eluent was concentrated in vacuo to obtain the desired product (482 mg, 25%): MS *m*/*z* = 466. ^{1}H NMR (DMSO-d_6) δ 12.13 (br s, 1H), 10.32 (s, 1H), 10.03 (s, 1H), 8.43 (d, *J* = 1.3 Hz, 1H), 8.16 (ddd, *J* = 8.9, 7.4, 2.8 Hz, 1H), 7.48 (s, 1H), 7.19–7.05 (m, 2H), 6.44 (dd, *J* = 4.4, 2.4 Hz, 1H), 6.29 (br s, 1H), 5.53–5.30 (m, 1H), 4.74 (d, *J* = 10.1 Hz, 1H), 3.95–3.67 (m, 2H), 2.76–2.27 (m, 2H), 1.74 (br s, 1H), 0.91–0.74 (m, 2H), 0.72–0.59 (m, 1H), 0.52 (br s, 1H).

4.1.13. (2*S*,4*S*)-1-(4-(5-Cyclopropyl-1*H*-pyrazol-3-ylamino) pyrrolo[1,2-*f*][1,2,4]triazin-2-yl)-4-fluoro-*N*-(pyrimidin-4-yl)pyrrolidine-2-carboxamide (11)

Starting with pyrimidin-4-amine, procedure B was followed with the addition of heating the reaction to 50 °C to provide the desired product (49%): MS *m*/*z* = 447 (neg. mode). ^{1}H NMR (DMSO-d_6) δ 12.05 (br s, 1H), 10.63 (s, 1H), 10.31 (s, 1H), 8.84 (d, *J* = 0.8 Hz, 1H), 8.64 (d, *J* = 5.8 Hz, 1H), 8.06 (d, *J* = 5.5 Hz, 1H), 7.45 (s, 1H), 7.13 (br s, 1H), 6.43 (dd, *J* = 4.3, 2.3 Hz, 1H), 6.31 (br s, 1H), 5.52–5.30 (m, 1H), 4.87 (d, *J* = 10.1 Hz, 1H), 3.93–3.71 (m, 2H), 2.77–2.53 (m, 1H), 2.53–2.35 (m, 1H), 1.71 (br s, 1H), 0.78 (d, *J* = 8.3 Hz, 2H), 0.67–0.46 (m, 2H).

4.1.14. (2*S*,4*S*)-1-(4-(5-Cyclopropyl-1*H*-pyrazol-3-ylamino) pyrrolo[1,2-*f*][1,2,4]triazin-2-yl)-4-fluoro-*N*-(5-methylthiazol-2-yl)pyrrolidine-2-carboxamide (12)

Starting with 5-methylthiazol-2-amine, procedure B was followed to provide the desired product (50%): MS *m*/*z* = 468. ^{1}H NMR (CD_3OD) δ 7.39 (dd, *J* = 2.5, 1.5 Hz, 1H), 7.00 (d, *J* = 1.3 Hz, 1H), 6.86–6.79 (m, 1H), 6.47 (dd, *J* = 4.5, 2.5 Hz, 1H), 6.16 (s, 1H), 5.46–5.27 (m, 1H), 4.92–4.84 (m, 1H), 4.05–3.91 (m, 1H), 3.90–3.71 (m, 1H), 2.68–2.50 (m, 2H), 2.35 (d, *J* = 1.3 Hz, 3H), 1.84–1.72 (m, 1H), 0.95–0.83 (m, 2H), 0.76–0.62 (m, 2H).

4.1.15. (2*S*,4*S*)-1-(4-(5-Cyclopropyl-1*H*-pyrazol-3-ylamino) pyrrolo[1,2-*f*][1,2,4]triazin-2-yl)-4-fluoro-*N*-(thiazol-2-yl)pyrrolidine-2-carboxamide (13)

Starting with thiazol-2-amine, procedure B was followed to provide the desired product (47%): MS *m*/*z* = 454. ^{1}H NMR (DMSO-d_6) δ 12.05 (br s, 1H), 12.00 (s, 1H), 10.26 (s, 1H), 7.44 (d, *J* = 3.7 Hz, 2H), 7.19 (d, *J* = 3.7 Hz, 1H), 7.13 (br s, 1H), 6.43 (br s, 1H), 6.25 (br s, 1H), 5.50–5.32 (m, 1H), 4.89 (d, *J* = 10.1 Hz, 1H), 3.96–3.72 (m, 2H), 2.75–2.34 (m, 2H), 1.72 (br s, 1H), 0.83 (d, *J* = 8.2 Hz, 2H), 0.73–0.56 (m, 2H).

4.1.16. (2*S*,4*S*)-1-(4-(5-Cyclopropyl-1*H*-pyrazol-3-ylamino) pyrrolo[1,2-*f*][1,2,4]triazin-2-yl)-4-fluoro-*N*-(1,2,4-thiadiazol-5-yl)pyrrolidine-2-carboxamide (14)

Isopropylmagnesium chloride (2.0 M/THF, 15.6 mL, 31.1 mmol) was slowly added to a solution of 1,2,4-thiadiazol-5-amine (3.15 g, 31.1 mmol) in DME (135 mL). After several minutes, (2*S*,4*S*)-methyl 1-(4-((5-cyclopropyl-1H-pyrazol-3-yl)amino)pyrrolo[2,1-f][1,2,4]triazin-2-yl)-4-fluoropyrrolidine-2-carboxylate (1.50 g, 3.89 mmol) was added. The reaction was stirred at 80 °C for 3 d. After cooling, the reaction was poured into sat aq NH_4Cl (200 mL) and extracted with EtOAc (200 mL, then 100 mL). The combined organics were washed with water (4 × 200 mL), dried ($MgSO_4$), filtered, and concentrated in vacuo. The residue was triturated in a small amount of MeOH, then 3:1 DMSO/MeOH to give product (825 mg, 46%): MS *m*/*z* = 455. ^{1}H NMR (DMSO-d_6) δ 13.08 (br s, 1H), 12.08 (br s, 1H), 10.30 (br s, 1H), 8.45 (s, 1H), 7.46 (br s, 1H), 7.13 (br s, 1H), 6.43 (dd, *J* = 4.2, 2.4 Hz, 1H), 6.13 (br s, 1H), 5.54–5.31 (m, 1H), 4.98 (d, *J* = 9.6 Hz, 1H), 3.99–3.67 (m, 2H), 2.84–2.58 (m, 1H), 2.56–2.37 (m, 1H), 1.72 (br s, 1H), 0.85 (d, *J* = 6.3 Hz, 2H), 0.73–0.53 (m, 2H).

4.1.17. (2*S*,4*R*)-1-(4-(5-cyclopropyl-1H-pyrazol-3-ylamino) pyrrolo[1,2-f][1,2,4]triazin-2-yl)-4-fluoro-N-(1,2,4-thiadiazol-5-yl)pyrrolidine-2-carboxamide (15)

Starting with the 1,2,4-thiadiazol-5-amine, procedure A was followed to provide the desired product (28% yield); MS: 455 $(M+H)^+$; 500 MHz ^{1}H NMR (d_6-DMSO) δ 13.15 (br s, 1H), 12.07 (br s, 1H), 10.26 (br s, 1H), 8.46 (s, 1H), 7.34 (br s, 1H), 7.11 (br s, 1H), 6.41 (br s, 1H), 6.31 (br s, 1H), 5.47 (d, 1H, *J* = 53.1 Hz), 4.96–4.81 (m, 1H), 4.15–3.99 (m, 1H), 3.97–3.77 (m, 1H), 2.82–2.66 (m, 1H), 2.39–2.20 (m, 1H), 1.90–1.78 (m, 1H), 0.99–0.83 (m, 2H), 0.80–0.66 (m, 2H).

4.1.18. (2*S*,4*S*)-1-(4-(5-Cyclopropyl-1*H*-pyrazol-3-ylamino) pyrrolo[1,2-*f*][1,2,4]triazin-2-yl)-4-fluoro-*N*-(5-fluorothiazol-2-yl)pyrrolidine-2-carboxamide (16)

In a sealable vial, a suspension of 5-fluorothiazol-2-amine, HCl (136 mg, 0.88 mmol) in toluene (0.6 mL) was cooled in an ice/salt bath. Triisobutylaluminum (1.0 M in toluene, 0.88 mL, 0.88 mmol) was slowly added. The reaction was warmed to rt, then (2*S*,4*S*)-methyl 1-(4-((5-cyclopropyl-1H-pyrazol-3-yl)amino)pyrrolo[2,1-f][1,2,4]triazin-2-yl)-4-fluoropyrrolidine-2-carboxylate (150 mg, 0.39 mmol) was added. The vial was sealed and heated to 50 °C overnight. After cooling, EtOAc (30 mL) and 0.25 M citric acid (30 mL) were added. The organics were dried ($MgSO_4$), filtered, and concentrated in vacuo. The residue was purified by preparative HPLC (Waters Atlantis 30 × 100 mm, 0–70% 9:1 [MeOH/H_2O 0.1% TFA]/1:9 [MeOH/H_2O 0.1% TFA]), then preparative chiral SFC (ChiralCel OJ-H, 30 × 250 mm, 17% MeOH/CO_2) to obtain the desired product (53 mg, 29%): MS *m*/*z* = 472. ^{1}H NMR (DMSO-d_6) δ 12.15 (s, 1H), 12.09 (br s, 1H), 10.29 (s, 1H), 7.45 (br s, 1H), 7.27 (d, *J* = 2.5 Hz, 1H), 7.12 (br s, 1H), 6.43 (dd, *J* = 4.3, 2.5 Hz, 1H), 6.22 (br s, 1H), 5.50–5.30 (m, 1H), 4.86 (d, *J* = 9.8 Hz, 1H), 3.93–3.68 (m, 2H), 2.76–2.53 (m, 1H), 2.47–2.31 (m, 1H), 1.76 (br s, 1H), 0.85 (d, *J* = 5.5 Hz, 2H), 0.74–0.58 (m, 2H).

4.1.19. (2*S*,4*S*)-1-(4-(5-Cyclopropyl-1*H*-pyrazol-3-ylamino) pyrrolo[1,2-*f*][1,2,4]triazin-2-yl)-4-fluoro-*N*-(pyrazin-2-yl)pyrrolidine-2-carboxamide (17)

Starting with pyridazin-4-amine, procedure B was followed except methylmagensium bromide was used instead of isopropylmagnesium chloride, to give the desired product (40%): MS *m*/*z* = 449. ^{1}H NMR (CD_3OD) δ 9.42 (d, *J* = 1.0 Hz, 1H), 8.29–8.23 (m, 2H), 7.44–7.36 (m, 1H), 6.84 (d, *J* = 3.5 Hz, 1H), 6.48 (dd, *J* = 4.3, 2.5 Hz, 1H), 6.24 (s, 1H), 5.48–5.28 (m, 1H), 4.88–4.79 (m, 2H), 4.05–3.90 (m, 1H), 3.90–3.71 (m, 1H), 2.73–2.49 (m, 2H), 1.81–1.67 (m, 1H), 0.93–0.79 (m, 2H), 0.72–0.52 (m, 2H).

4.2. Cellular assays

Cell line identity of A549 and HCT-116 has been confirmed by genotyping on the Affymetrix SNP6 array and comparison to data generated by the COSMIC project.[20] Cellular proliferation assays based on incorporation of 3H-thymidine (GE Healthcare) were performed at 72 h as described.[8] Experimental design, cell growth and treatment for expression profiling analysis was as described:[12] compounds were dosed for four hours at 12 concentrations from 170 pM to 30 μM (a three-fold dilution series covering a six logarithm range).

4.3. Profiling assays

Kinase selectivity profile assays were performed at Ambit Biosciences on the KINOMEScan platform[10] using compounds at 1 μM. Affymetrix transcriptional profile analysis was as described;[12] briefly, manufacturer's protocols were used to prepare RNA using the RNeasy Mini Kit (Qiagen), to evaluate RNA integrity, cRNA synthesis and cRNA fragmentation on a Bioanalyzer 2100 (Agilent Technologies), to process 2.5 μg of total RNA for hybridization on the HT_HG-U133A array, and to scan arrays with a GCS3000 scanner (Affymetrix). The cel files were processed together using the robust multi-array analysis (RMA) algorithm.[21] See Supplementary Figure S1 and Table S4 for quality control data. The 22,283 probesets on the HG-133A array were mapped to 12,642 loci using the criterion of >80% sequence identity to the loci annotated in NCBI's RefSeq database, release 40.[22]

4.4. In vivo tumor models

Antitumor activity in the xenograft model HCT-116 was determined as previously described.[8] Dosing regimen was QD for 14 days in PEG400/water, 80:20.

4.5. Statistical analysis and display

Kinase phylogeny was taken from the trees built by Manning et al.[23] The trees were rendered as 'tumbleweeds', which preserve tree structure and edge length while distributing the edges in a circular layout to improve separation of leaf nodes.

The SDRS algorithm, which performs a grid search to identify parameters giving the best fit to a sigmoidal dose response curve, was applied as previously described,[12] with the modification that a 1.1 multiple and no step function was used to set the 128 log-evenly distributed test values for C. The 'response heatmap' (Fig. 2) was generated from all 128 SDRS lists, which contain the lowest *P* value for each probeset at each of the test values. First, we performed a trim of variables with low signal: for each treatment, results for the probesets in the bottom 55% of expression values were not used. This resulted in exclusion of the c. 12000 probesets whose highest value in the treatment dataset did not exceed 3-fold of background signal. Then, in each list, the number of probesets whose *P* value passed an FDR cutoff was calculated using 1% increments from FDR = 1% to FDR = 35%, resulting in a 35 × 128 matrix.

For visualization of expression profiling data on heatmaps, the twelve intensity values for each treatment (ten for compound **15**) were scaled from zero to 1, providing a view of the direction and consistency of change for each probeset. Note that where a consistent dose response is not present, this scaling results in a random pattern of high and low values across the dose series. The scaling may also result in a dose response being apparent for

probesets where the criteria for response transcripts (i.e., fold-change and fit to a sigmoidal curve) were not met. All heatmaps use the hierarchical clustering function of Partek Discovery Suite, performed with euclidean distance metrics applied to the scaled data.

Gene set enrichment was performed using the hypergeometric distribution (Fisher's exact test), expressed as a single-tailed *p*-value. Tested ontology sets included the three categories from GO (biological process, cellular component, molecular function[14]), the Conserved Domain Database, MSigDB[15] and Interpro families. Within each ontology set, Bonferroni correction was applied proportional to the number of ontology terms considered.

Supplementary data

Supplementary data associated with this article can be found, in the online version, at doi:10.1016/j.bmc.2011.10.090.

References and notes

1. Jia, Y.; Quinn, C. M.; Kwak, S.; Talanian, R. V. *Curr. Drug. Discov. Technol.* **2008**, *5*, 59.
2. Lamb, J.; Crawford, E. D.; Peck, D.; Modell, J. W.; Blat, I. C.; Wrobel, M. J.; Lerner, J.; Brunet, J. P.; Subramanian, A.; Ross, K. N.; Reich, M.; Hieronymus, H.; Wei, G.; Armstrong, S. A.; Haggarty, S. J.; Clemons, P. A.; Wei, R.; Carr, S. A.; Lander, E. S.; Golub, T. R. *Science* **2006**, *313*, 1929.
3. Talpaz, M.; Shah, N. P.; Kantarjian, H.; Donato, N.; Nicoll, J.; Paquette, R.; Cortes, J.; O'Brien, S.; Nicaise, C.; Bleickardt, E.; Blackwood-Chirchir, M. A.; Iyer, V.; Chen, T. T.; Huang, F.; Decillis, A. P.; Sawyers, C. L. N. *Engl. J. Med.* **2006**, *354*, 2531.
4. Araujo, J.; Logothetis, C. *Cancer Treat Rev.* **2010**, *36*, 492.
5. Hammerman, P. S.; Sos, M. L.; Ramos, A. H.; Xu, C.; Dutt, A.; Zhou, W.; Brace, L. E.; Woods, B. A.; Lin, W.; Zhang, J.; Deng, X.; Lim, S. M.; Heynck, S.; Peifer, M.; Simard, J. R.; Lawrence, M. S.; Onofrio, R. C.; Salvesen, H. B.; Seidel, D.; Zander, T.; Heuckmann, J. M.; Soltermann, A.; Moch, H.; Koker, M.; Leenders, F.; Gabler, F.; Querings, S.; Ansén, S.; Brambilla, E.; Brambilla, C.; Lorimier, P.; Brustugun, O. T.; Helland, Å.; Petersen, I.; Clement, J. H.; Groen, H.; Timens, W.; Sietsma, H.; Stoelben, E.; Wolf, J.; Beer, D. G.; Tsao, M. S.; Hanna, M.; Hatton, C.; Eck, M. J.; Janne, P. A.; Johnson, B. E.; Winckler, W.; Greulich, H.; Bass, A. J.; Cho, J.; Rauh, D.; Gray, N. S.; Wong, K.-K.; Haura, E. B.; Thomas, R. K.; Meyerson, M. *Cancer Discov.* **2011**, *1*, 78.
6. Zou, H. Y.; Li, Q.; Lee, J. H.; Arango, M. E.; McDonnell, S. R.; Yamazaki, S.; Koudriakova, T. B.; Alton, G.; Cui, J. J.; Kung, P.-P.; Nambu, M. D.; Los, G.; Bender, S. L.; Mroczkowski, B.; Christensen, J. G. *Cancer Res.* **2007**, *67*, 4408.
7. Kwak, E. L.; Bang, Y.-J.; Camidge, D. R.; Shaw, A. T.; Solomon, B.; Maki, R. G.; Ou, S.-H. I.; Dezube, B. J.; Jänne, P. A.; Costa, D. B.; Varella-Garcia, M.; Kim, W.-H.; Lynch, T. J.; Fidias, P.; Stubbs, H.; Engelman, J. A.; Sequist, L. V.; Tan, W.; Gandhi, L.; Mino-Kenudson, M.; Wei, G. C.; Shreeve, S. M.; Ratain, M. J.; Settleman, J.; Christensen, J. G.; Haber, D. A.; Wilner, K.; Salgia, R.; Shapiro, G. I.; Clark, J. W.; Iafrate, A. J. *N. Eng. J. Med.* **2010**, *363*, 1693.
8. Carboni, J. M.; Wittman, M.; Yang, Z.; Lee, F.; Greer, A.; Hurlburt, W.; Hillerman, S.; Cao, C.; Cantor, G. H.; Dell-John, J.; Chen, C.; Discenza, L.; Menard, K.; Li, A.; Trainor, G.; Vyas, D.; Kramer, R.; Attar, R. M.; Gottardis, M. M. *Mol. Cancer Ther.* **2009**, *8*, 3341.
9. Wittman, M. D.; Carboni, J. M.; Yang, Z.; Lee, F. Y.; Antman, M.; Attar, R.; Balimane, P.; Chang, C.; Chen, C.; Discenza, L.; Frennesson, D.; Gottardis, M. M.; Greer, A.; Hurlburt, W.; Johnson, W.; Langley, D. R.; Li, A.; Li, J.; Liu, P.; Mastalerz, H.; Mathur, A.; Menard, K.; Patel, K.; Sack, J.; Sang, X.; Saulnier, M.; Smith, D.; Stefanski, K.; Trainor, G.; Velaparthi, U.; Zhang, G.; Zimmermann, K.; Vyas, D. M. *J. Med. Chem.* **2009**, *52*, 7360.
10. Karaman, M. W.; Herrgard, S.; Treiber, D. K.; Gallant, P.; Atteridge, C. E.; Campbell, B. T.; Chan, K. W.; Ciceri, P.; Davis, M. I.; Edeen, P. T.; Faraoni, R.; Floyd, M.; Hunt, J. P.; Lockhart, D. J.; Milanov, Z. V.; Morrison, M. J.; Pallares, G.; Patel, H. K.; Pritchard, S.; Wodicka, L. M.; Zarrinkar, P. P. *Nat. Biotech.* **2008**, *26*, 127.
11. Lolli, G.; Johnson, L. N. *Cell Cycle* **2005**, *4*, 572.
12. Ji, R. R.; de Silva, H.; Jin, Y.; Bruccoleri, R. E.; Cao, J.; He, A.; Huang, W.; Kayne, P. S.; Neuhaus, I. M.; Ott, K. H.; Penhallow, B.; Cockett, M. I.; Neubauer, M. G.; Siemers, N. O.; Ross-Macdonald, P. *PLoS Comput. Biol.* **2009**, *5*, e1000512.
13. Tilford, C. A.; Siemers, N. O. In *Protein Networks and Pathway Analysis*; Nikolsky, Y., Bryant, J., Eds.; Humana Press, 2009; vol. 563, p 99.
14. Ashburner, M.; Ball, C. A.; Blake, J. A.; Botstein, D.; Butler, H.; Cherry, J. M.; Davis, A. P.; Dolinski, K.; Dwight, S. S.; Eppig, J. T.; Harris, M. A.; Hill, D. P.; Issel-Tarver, L.; Kasarskis, A.; Lewis, S.; Matese, J. C.; Richardson, J. E.; Ringwald, M.; Rubin, G. M.; Sherlock, G. *Nat. Genet.* **2000**, *25*, 25.
15. Subramanian, A.; Tamayo, P.; Mootha, V. K.; Mukherjee, S.; Ebert, B. L.; Gillette, M. A.; Paulovich, A.; Pomeroy, S. L.; Golub, T. R.; Lander, E. S.; Mesirov, J. P. *Proc. Nat. Acad. Sci.* **2005**, *102*, 15545.
16. Lachmann, A.; Ma'ayan, A. *Bioinformatics* **2009**, *25*, 684.
17. Kruse, U.; Pallasch, C. P.; Bantscheff, M.; Eberhard, D.; Frenzel, L.; Ghidelli, S.; Maier, S. K.; Werner, T.; Wendtner, C. M.; Drewes, G. *Leukemia* **2011**, *25*, 89.
18. Lam, L.; Pickeral, O.; Peng, A.; Rosenwald, A.; Hurt, E.; Giltnane, J.; Averett, L.; Zhao, H.; Davis, R. E.; Sathyamoorthy, M.; Wahl, L.; Harris, E.; Mikovits, J.; Monks, A.; Hollingshead, M.; Sausville, E.; Staudt, L. *Genome Biol.* **2001**, *2*. research0041.1.
19. Ross-Macdonald, P.; de Silva, H.; Guo, Q.; Xiao, H.; Hung, C. Y.; Penhallow, B.; Markwalder, J.; He, L.; Attar, R. M.; Lin, T. A.; Seitz, S.; Tilford, C.; Wardwell-Swanson, J.; Jackson, D. *Mol. Cancer Ther.* **2008**, *7*, 3490.
20. Forbes, S. A.; Bhamra, G.; Bamford, S.; Dawson, E.; Kok, C.; Clements, J.; Menzies, A.; Teague, J. W.; Futreal, P. A.; Stratton, M. R. *Curr. Protoc. Hum. Genet.* **2008**, 11. Chapter 10.
21. Irizarry, R. A.; Warren, D.; Spencer, F.; Kim, I. F.; Biswal, S.; Frank, B. C.; Gabrielson, E.; Garcia, J. G.; Geoghegan, J.; Germino, G.; Griffin, C.; Hilmer, S. C.; Hoffman, E.; Jedlicka, A. E.; Kawasaki, E.; Martinez-Murillo, F.; Morsberger, L.; Lee, H.; Petersen, D.; Quackenbush, J.; Scott, A.; Wilson, M.; Yang, Y.; Ye, S. Q.; Yu, W. *Nat. Methods* **2005**, *2*, 345.
22. Pruitt, K. D.; Tatusova, T.; Maglott, D. R. *Nucleic Acids Res.* **2007**, *35*, D61.
23. Manning, G.; Whyte, D. B.; Martinez, R.; Hunter, T.; Sudarsanam, S. *Science* **2002**, *298*, 1912.